A Metal Attenuation Study on Waste Rock Collected from the East Dump, Antamina Mine, Peru: A Combined Mineralogical and Geochemical Approach

Laura Laurenzi, K. Ulrich Mayer and Roger Beckie

Department of Earth, Ocean and Atmospheric Sciences, University of British Columbia, Canada

ABSTRACT

In this study we evaluate the influence of secondary minerals on metal attenuation using a suite of geochemical and mineralogical tests on three samples collected from different depths in the East Dump, Antamina Mine in Peru. The bulk elemental content and mineralogy are determined using trace metal analysis by inductively coupled plasma mass spectrometry (ICP-MS) after digestion and X-Ray Diffraction (XRD), respectively. A sequential extraction procedure (SEP) is used to identify the phases associated with the metals. Optical mineralogy and scanning electron/back-scatter electron microscopy (SEM/BSE) are used to identify secondary mineral phases, elements associated with the secondary minerals and the mode of occurrence of the secondary minerals.

Precipitation of weak-acid soluble phases and sorption/co-precipitation with amorphous reducible phases are the predominant attenuation mechanisms for the metals studied (i.e., arsenic, copper, lead, molybdenum and zinc). Copper, lead, and zinc are associated with weak-acid soluble phases and reducible phases. Arsenic and molybdenum are associated with reducible phases. Iron oxides are the predominant reducible phases forming coatings around sulfides and silicate minerals, or discrete mineral grains. Metal carbonates/sulfates (with variable Cu and Zn content) and zinc silicates are the predominant weak-acid soluble phases forming coatings on calcium carbonates and silicate grains, or as discrete mineral grains. This combined mineralogical and geochemical approach elucidates the nature of secondary minerals and associated metal attenuation processes.

Keywords: Metal Attenuation, Waste rock, Geochemistry, Mineralogy

INTRODUCTION

Mine waste rock often contains sulfide minerals that oxidize when exposed to oxygen and water. Without sufficient carbonate mineral buffering capacity in the waste rock, acidic conditions can develop leading to acid rock drainage (ARD); however, if the waste rock contains sufficient carbonate minerals to buffer the acidity generated by the oxidation of sulfides, neutral conditions can persist resulting in neutral rock drainage (NRD). Dissolved metal concentrations differ in ARD and NRD because metal mobility is highly dependent on pH. In ARD, Al, Fe, Cu, Pb, Zn, Cd, Mn, Co, and Ni are generally mobile (Al et al., 2000), while in NRD metals which are either weakly hydrolyzing such as Zn, Ni or oxyanion forming such as Mo, As, Se, and Cr are generally mobile (Price, 2009). This is because in NRD, cationic trace metals can be sequestered in secondary mineral phases and sorbed onto metal (oxy)hydroxides and clay minerals (Smith, 1999; Al et al., 2000). Oxyanions are more mobile in NRD because sorption onto iron oxides increases as pH drops below neutral. Thus, secondary minerals are an important control on the quality of water emanating from waste materials (van der Sloot and van Zomeren 2012; Al et al., 2000). Understanding the mechanisms that attenuate metals from waste rock is essential for reliable predictions of water quality (Mayer et al., 2003; Al et al., 2000). The objective of this study is to identify the secondary minerals and processes that attenuate metals by examining samples collected from the full scale operating waste dump, the East Dump at the Antamina Mine, Peru. Results from this study can be compared to the results of laboratory and smaller scale tests also conducted on waste rock material from this site.

METHODOLOGY

Project Site and Sample Collection

The Antamina deposit is a copper-zinc-molybdenum skarn formed by the intrusion quartz monzonite into limestone (Lipten & Smith, 2004; Love et al., 2004; Redwood, 1999). Waste is subdivided into classes based on the criteria summarized in Table 1. The East Dump, the focus of this study, receives all classes of waste rock and is therefore geochemically heterogeneous.

Table 1 Antamina Waste Rock Classification System

Class	Description	Zn	As	Sulfide
A	(Exo,Endo)skarn, intrusive, hornfels, Marbles Limestone	>1500 ppm	>400 ppm	> 3%
B	Hornfels, marble, limestone	700-1500 ppm	N/A	<2-3%
C	Hornfels, marble, limestone	<700 ppm	<400 ppm	<2-3%

The waste rock samples used for this study were collected from two boreholes at site BH-1 drilled using a reverse circulation drill rig. At the time of drilling, the deepest material in East Dump had been in place for over ten years, while the shallowest material for more than 5 years. Composite samples of waste rock material (at 1.5 m intervals) were collected and sieved using a 2 mm (#10) mesh. Sixteen samples were initially characterized for bulk elemental content, X-ray Diffraction (XRD) and sequential extraction procedure (SEP) testing, the results of which were used to focus scanning electron/back-scatter electron microscopy (SEM/BSE) tests on three samples. The results of the geochemical and mineralogical testing on the three samples are discussed here.

Testing Framework

The bulk elemental content of the samples was determined using ICP-MS analysis after a 4-acid digestion by SGS in Vancouver, Canada. XRD was used to identify crystalline minerals. XRD data were collected using a Bruker D8 Focus Diffractometer with a scanning step of 0.029° 2θ and counting time of 100.1 s/ over a range of 3-80° 2θ. While XRD is useful for crystalline mineral phases, XRD cannot identify minerals below ~1% abundance or those that are amorphous or nano-crystalline. Accordingly, the sequential extraction procedure (SEP) proposed by Hall et al. (1996) (

Table 2) was used to identify the predominant secondary phases and attenuation mechanisms for As, Cu, Mo, Pb, and Zn.

Three samples that showed elevated metal concentrations in the SEP were investigated in more detail. Thin sections of these three samples were prepared and examined using transmitted/reflected light microscopy where individual mineral grains were targeted for SEM/BSE imaging and Electron Dispersion Spectra (EDS) analysis. For the SEM/BSE analysis, the thin sections were coated with evaporated carbon and examined on a Philips XL30 SEM equipped with Bruker Quantax 200 Microanalysis system and light element XFLASH 4010 Silicon Drift detector. Semi-quantitative analysis of the EDS yielded weight percent (wt.%) of elements associated with the secondary minerals.

Table 2 Sequential extraction procedure used on samples (Hall et al., 1996)

Step	Phases	Method[1]
1	Water Soluble	50 mL deionized water shake for 1h at room temperature
2	Weakly sorbed /Exchangeable[2]	40 mL 1M $MgCl_2$ shake for 1 hour at room temperature
3	Weak-acid soluble	20 mL 1M CH_3COONa (sodium acetate) at pH 5 shake for 6h centrifuge for 10min Repeat Step
4	Amorphous reducible phases	20 mL 0.25M $NH_2OH*HCl$ (hydroxylamine hydrochloride) in 0.25 HCl place in 60^0C water bath for 2h every 30min vortex contents Repeat Step but heat for only 30 min
5	Crystalline reducible phases	30 mL of 1 M $NH_2OH*HCl$ (hydroxylamine hydrochloride) in 25% CH_3COOH (acetic acid) place in 90^0C water bath for 3h, vortex every 20 min Repeat Step but heat for only 1.5 hours
6	Residual Phases	4 - Acid Digest[3]

NOTES:

(1) Steps 3 – 5 are repeated using the same liquid solid ratio (LSR). Leachates are analyzed separately and the concentrations are summed.

(2) Weakly sorbed/exchangeable step taken from (Tessier et al., 1979)

(3) Residual fraction was determined by 4-acid digest at SGS, Burnaby (BC, Canada)

Results

From the lithologic logs produced at the time of drilling (not shown), samples BH-1s (1.5 – 3.0) and BH-1d (90.0 – 91.5) are composed predominantly of marble and marble diopside lithologies. Both samples contain some skarn while BH-1d (90.0 – 91.5) also contains some igneous intrusive rock. BH-1d (19.5 – 21.0) is predominantly igneous intrusive, with some marble.

The bulk elemental content of As, Cu, Mo, Pb, and Zn are presented in Table 3. Among the three samples, BH-1s (1.5 – 3.0) has the highest content of Mo and Pb and BH-1d (19.5 – 20.0) and BH-1d (90.0 – 91.5) have the higher Cu and Zn. Total arsenic is highest in BH-1d (90.0 – 91.5).

Table 3 Total metal concentrations for select elements

	Units	BH-1s (1.5 - 3.0)	BH-1d (19.5 - 21.0)	BH-1d (90.0 - 91.5)
As	ppm	104	49	118
Cu	ppm	1340	5740	5530
Mo	ppm	468	104	73.3
Pb	ppm	2080	195	593
Zn	ppm	674	4900	>10000

Generally, the primary mineralogy of the samples is consistent with the primary lithology of the samples, which includes quartz, orthoclase, albite, biotite, actinolite and calcite in all samples. Diopside, garnets, and vesuvianite were additionally found in marble diopside and skarn bearing samples, BH-1s (1.5 – 3.0) and BH-1d (90.0 – 91.5). Table 4 summarizes the sulfide and secondary mineralogy of the samples determined from XRD. The secondary minerals noted in the XRD are chlorite, gypsum, smithsonite, otavite, wulfenite, and hemimorphite. In addition there was a strong amorphous background in the diffraction patterns, indicative of amorphous minerals such as iron oxides and aluminum hydroxides. Although hemimorphite is a secondary mineral that could form in the dump due to the weathering of Zn bearing sulfides, it is also part of the supergene mineralization of the Antamina deposit (Personal communication 2013, L. Plascencia). Wulfenite found in the XRD of samples from site BH-1 (not shown here) confirms previous work using batch and field experiments that indicate that Mo precipitation is likely in the form of wulfenite (Hirsche et al. 2012; Conlan 2009).

Table 4 Mineralogy as determined by XRD

Mineral	Chemical Formula	BH-1s (1.5 - 3.0)	BH-1d (19.5 - 21.0)	BH-1d (90.0 - 91.5)
Sulfides				
Pyrite	FeS_2	x	x	x
Molybdenite	MoS_2	x		
Chalcopyrite	$CuFeS_2$		x	x
Secondary minerals				
Chlorite	$(Mg,Fe)_3(Si,Al)_4O_{10}(OH)_2 \cdot (Mg,Fe)_3(OH)_6$	x	x	x
Gypsum	$CaSO_4$	x	x	x
Smithsonite	$ZnCO_3$		x	x
Otavite	$CdCO_3$			x
Hemimorphite	$Zn_4Si_2O_7(OH)_2 \cdot H_2O$			x
Amorphous Background	n/a	x	x	x

Sequential Extraction Procedure

Figure 1 presents the SEP results for As, Cu, Mo, Pb and Zn. Only Ca and S were found in the water soluble leach step (step 1) and indicate that gypsum is the only water-soluble phase. Table 5 presents the range in concentrations extracted (in µg) for the SEP steps 2 – 5 and the % extracted for each step when compared to the total amount extracted from the SEPs. From Table 5, weak-acid soluble phases and amorphous reducible phases are considered attenuation mechanisms for Cu, Pb, and Zn and reducible phases are considered to have some attenuating control on As and Mo.
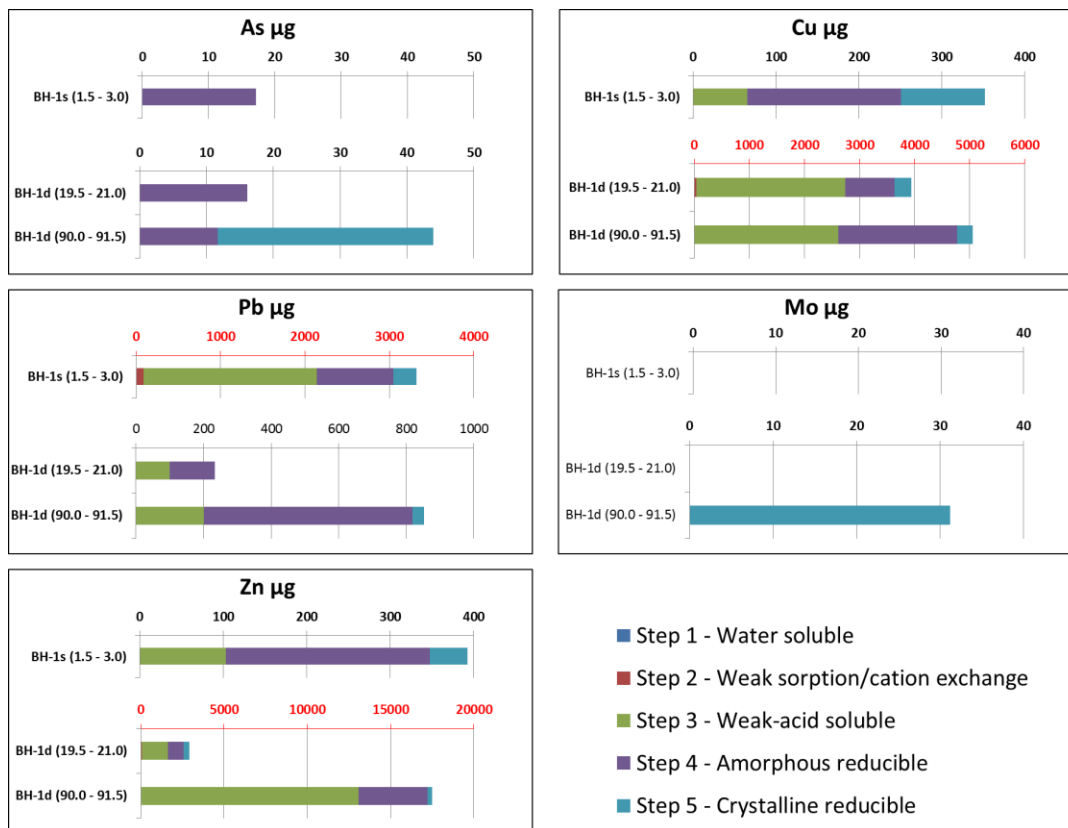
Figure 1 Sequential extraction results for select elements in µg as leached from a 1g sample. Each sub-figure has the same scale unless otherwise indicated using red text

Table 5 SEP results in ppm and % for steps 2 - 5

|	As	Cu	Mo	Pb	Zn
step 2 - Weak sorption/cation exchange					
µg extracted	-	DL – 34.6	-	DL – 90.0	DL – 44.7
% extracted[1]	-	0 - 0.65	-	0 – 2.66	0 - 0.96
step 3 - Weak-acid soluble					
µg extracted	-	65.4 – 2707.5	-	99.8 – 2048.4	103.4 – 13081.1
% extracted[1]	-	6 – 51.0	-	23.1 – 60.4	13.7 – 72.2
step 4 - Amorphous reducible					
µg extracted	0.4 - 0.6	185.2 – 2156.9	-	133.8 – 906.3	243.9 – 4125.9
% extracted[1]	12.0 – 49.3	16.9 – 37.8	-	26.7 – 70.8	20.1- 32.2
step 5 - Crystalline reducible					
µg extracted	DL – 32.3	101.1 – 298.9	DL – 31.2	DL – 280.0	45.4 – 365.5
% extracted[1]	0.0 – 33.3	4.8 – 9.2	0.0 – 62.6	0.0 – 8.3	1.6 – 7.7

Notes:

(1) % extracted compared to the total extracted from all steps of the SEP
(2) DL – indicates that concentrations were below detection limit and mass extracted was not calculated

Optical Microscopy and SEM/BSE imaging

Weak-acid Soluble Phases

Figure 2 to Figure 4 present transmitted light microscopy and SEM/BSE images for mineral grains suspected of contributing to Cu and Zn found in the weak-acid soluble leach step. Carbon is included in the semi-quantitative analyses in these figures because it is suspected that these secondary minerals are either carbonates or sulfates or some carbonate/sulfate mix and that the carbon coating used in the method preparation would not contribute significantly to the results. Figure 2 shows two distinct mineral coatings a dark black Zn/Cu carbonate, and a blue/green Cu/Zn carbonate/sulfate coating a silicate/carbonate mineral grain. Figure 3 shows a Cu/Zn carbonate mineral associated with hemimorphite. Figure 4 shows a discrete Zn/Cu carbonate mineral grain. A weak-acid soluble secondary mineral with Pb association was not found although SEP leachate results indicate that this is a potential attenuation mechanism for Pb. These results indicate that more than one Cu/Zn weak-acid soluble phase is forming. In addition, hemimorphite ($Zn_4Si_2O_7(OH)_2 \cdot H_2O$) dissolved in the weak-acid used for this step (Laurenzi, unpublished).
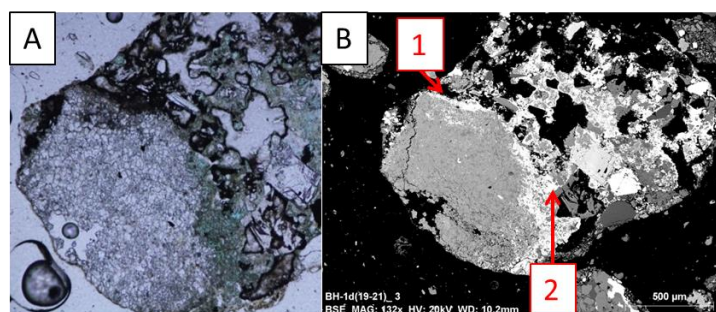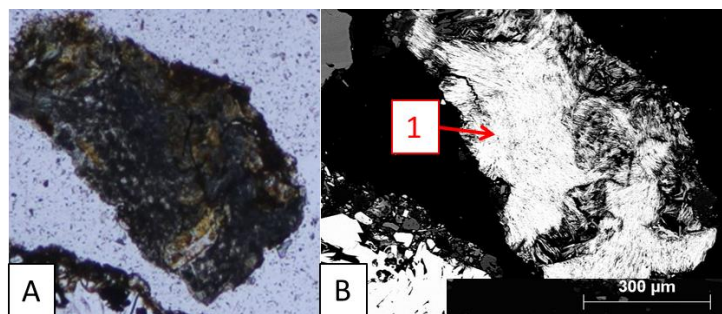

Figure 2 A) Plane-polarized transmitted light photograph of silicate/calcite mineral with black and blue/green secondary mineral coating. B) SEM/BSE image of same mineral: 1) black mineral semi-quantitative analysis; 9 wt.% Cu, 28 wt.% Zn, 22 wt.% O, 8 wt.% C, 0.2 wt.% S.; 2) blue/green mineral semi-quantitative analysis; 46 wt.% Cu, 1.5 wt.% Zn, 15 wt.% O, 5 wt.% C, 6 wt.% S
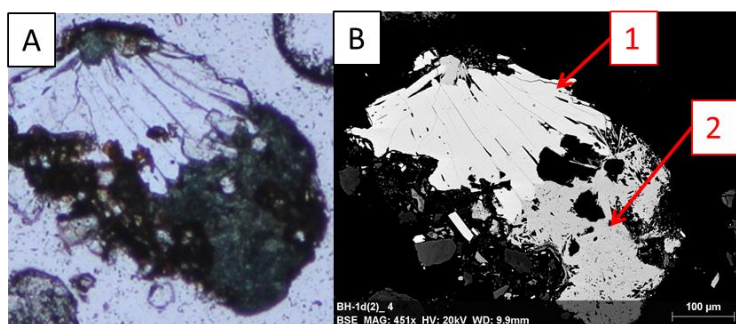
Figure 3 A) Plane-polarized transmitted light photograph of zinc silicate mineral (hemimorphite) with blue/green secondary mineral coating. B) SEM/BSE image of mineral: 1) Hemimorphite semi-quantitative analysis; 50 wt.% Zn, 16 wt.% O, 9 wt.% Si, 2 wt.% C. 2) blue/green mineral semi-quantitative analysis; 42 wt.% Cu, 13 wt.% Zn, 23 wt.% O, 9 wt.% C
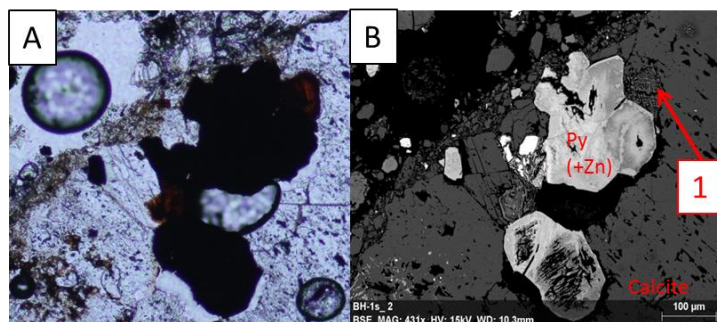
Figure 4 A) Plane-polarized transmitted light photograph of mineral. B) SEM/BSE image of same mineral: 1) mineral semi-quantitative analysis; 18 wt.% Cu, 32 wt.% Zn, 18 wt.% O, 10 wt.% C

Amorphous Reducible Phases

The predominant reducible phases are iron oxides. Figure 5 to Figure 6 present transmitted light and SEM/BSE images for iron oxides found in the samples. The iron oxides form as coatings around sulfide minerals, silicate minerals and as discrete mineral grains (not shown here). Iron oxides were found in all samples and contained variable concentrations of Cu (0.0 wt.% - 2.0 wt.%), Pb (0.0 wt.% - 4 wt.%), and (1wt.% - 7wt.%) Zn. The iron oxide in Figure 6 was determined to have 0.1 wt.% Mo.

Although As associations were not identified using SEM/BSE, the results of the SEP indicate that the As and Mo concentration may be below the detection limits of the SEM/BSE instrument. Sorption and co-precipitation onto these reducible phases is assumed to be one of the attenuation mechanisms for these metals.

Figure 5 A) Plane-polarized transmitted light photograph of pyrite mineral with iron oxide coatings. B) SEM/BSE image of same mineral. Semi-quantitative analysis of iron oxide 1) 28 wt.% Fe, 21 wt.% O, 1 wt.% Zn, 4 wt.% Pb
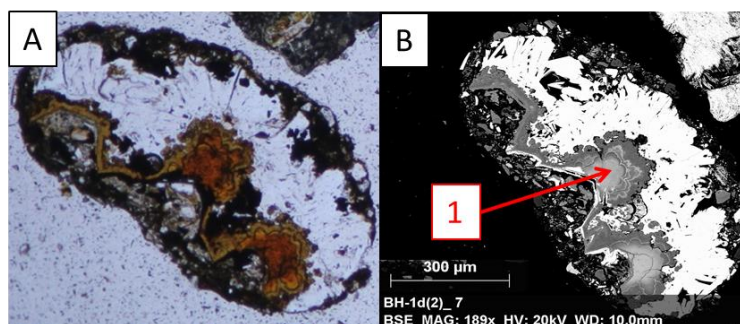
Figure 6 A) Plane-polarized transmitted light photograph of iron oxide coating hemimorphite (white mineral). B) SEM/BSE image of same mineral. Semi-quantitative analysis of iron oxide 1) 41 wt.% Fe, 26 wt.% O, 8 wt.% Zn, 2 wt. % Cu, 2 wt. % Pb, 0.01 wt. % Mo

DISCUSSION

The geochemical and mineralogical testing framework shows that weak-acid soluble and amorphous reducible phases are the predominant attenuation processes for Cu, Pb, and Zn. The main weak-acid soluble phases are copper and zinc bearing; however, their composition determined by SEM/BSE is not indicative of a single mineral phase. This supports field - experimental pile scale conclusions, that identified a blue (mostly amorphous copper sulfate) precipitate containing some malachite in a pile composed of Class A intrusive material (Peterson 2014). More work is required to determine the mineralogy of these weak-acid soluble phases. Hemimorphite, potentially a secondary mineral that formed in the East Dump, should also be considered a weak-acid soluble phase in which Zn is attenuated. The main reducible phases are iron oxides and can contain as much as 2.0 wt.% Cu, 4 wt.% Pb and 7 wt.% Zn. The variability in metals associated with the iron oxides is considered to be due to differences in the total metal content in the waste rock, flow patterns within the pile and the release rate of these metals from the waste rock. Low concentrations of As and Mo are associated with reducible phases dissolved in the SEP leachates. For As these associations were not identified in the SEM/BSE investigation possibly due to low content. While for Mo, sorption onto iron oxides, as determined from the SEP and SEM/BSE investigations, and precipitation of wulfenite, identified by XRD, are the likely attenuation processes. Based upon the results of the SEP, a lead-bearing weak-acid soluble phase was expected but was not identified in the mineralogical and SEM/BSE investigations. More work is required to identify the attenuating mechanism for lead. The metal/mineral associations seen in this study are considered to be the results of pore waters high in Zn and Cu and SO_4 and CO_3, from which Cu-Zn bearing minerals are precipitating. Due the presence of calcite in the samples the pH of the water is suspected to be near neutral, thus limiting the sorption of As and Mo.

CONCLUSION

This work focused on 3 samples collected from depth in an operational waste rock pile. This study highlights the benefit of detailed mineralogical and geochemical investigations to constrain metal attenuation phases and processes. It is important to examine samples collected from the field to support inferences made from laboratory tests.

Results from the SEP, microscopy and SEM/BSE investigations indicate that precipitation of weak-acid soluble phases and sorption onto amorphous reducible phases are the predominant attenuation mechanism for Cu, Pb and Zn. Cu and Zn are associated together with variable concentrations in weak-acid soluble phases. SEP tests show that Pb is being attenuated in a weak-acid soluble phase; however, this phase was not identified in the mineralogy or SEM/BSE work. SEP tests indicate that As is associated with reducible phases. SEP leachates and XRD tests indicate that Mo attenuation is via sorption onto iron oxides and precipitation of wulfenite, respectively.

ACKNOWLEDGEMENTS

References

Al, T. A., C. J. Martin, and D. W. Blowes. 2000. "Carbonate-Mineral/water Interactions in Sulfide-Rich Mine Tailings." *Geochimica Et Cosmochimica Acta* 64 (December): 3933–48.

Conlan, Michael Joseph William. 2009. "Attenuation Mechanisms for Molybdenum in Neutral Rock Drainage". University of British Columbia.

Hall, G.E.M., J.E. Vaive, R. Beer, and M. Hoashi. 1996. "Selective Leaches Revisited, with Emphasis on the Amorphous Fe Oxyhydroxide Phase Extraction." *Journal of Geochemical Exploration* 56: 59 –78.

Hirsche, Dustin Trevor, R. D. Beckie, Michael J. W. Conlan, Sharon Blackmore, J. L. Smith, B. Klein, K. Ulrich Mayer, C. A. Aranda, Luis A. Rojas Bardón, and Raúl Jamanca Castañeda. 2012. "Stacked Field Cells as a Means for Studying Metal Attenuation by Waste Rock Mixing at the Antamina Mine in Peru." In *Proceedings Ninth International Conference on Acid Rock Drainage*, 9. Ottawa, Canada.

Mayer, K. Ulrich, D. W. Blowes, and E.O. Frind. 2003. "Advances in Reactive-Transport Modelling of Contaminant Release and Attenuation from Mine-Waste Deposits." In *Environmental Aspects of Mine Wastes*. Vol. 31. Mineralogical Association of Canada Short Course Series (eds. Jambor, J.L.,Blowes, D.W., Ritchie, A.I.M.

Peterson, H. E. 2014. "Unsaturated Hydrology, Evaporation, and Geochemistry of Neutral and Acid Rock Drainage in Highly Heterogeneous Mine Waste Rock at the Antamina Mine, Peru."

Price, William A. 2009. "Prediction Manual for Drainage Chemistry from Sulphidic Geologic Materals."

Smith, K.S. 1999. "Metal Sorption on Mineral Surfaces: An Overview with Examples Relating to Mineral Deposits." In *The Environmental Geochemistry of Mineral Deposits*, edited by G.S. Plumlee and M.J. Logsdon. Society of Economic Geologists.

Van der Sloot, Hans Albert, and Andre van Zomeren. 2012. "Characterisation Leaching Tests and Associated Geochemical Speciation Modelling to Assess Long Term Release Behaviour from Extractive Wastes." *Mine Water and the Environment* 31 (2): 92–103. doi:10.1007/s10230-012-0182-8.